universe

MDPI

Article

Dynamics and Stability of the Two-Body Problem with Yukawa Correction to Newton's Gravity, Revisited and Applied Numerically to the Solar System

Nawras Abo Hasan [1,†], Nabil Joudieh [1,†] and Nidal Chamoun [2,*,†]

[1] Physics Department, Damascus University, Damascus P.O. Box 30621, Syria
[2] Physics Department, HIAST, Damascus P.O. Box 31983, Syria
* Correspondence: nchamoun@th.physik.uni-bonn.de
† These authors contributed equally to this work.

Abstract: In this manuscript, we review the motion of a two-body celestial system (planet–sun) for a Yukawa-type correction on Newton's gravitational potential using Hamilton's formulation. We reexamine the stability using the corresponding linearization Jacobian matrix, and verify that the conditions of Bertrand's theorem are met for radii $\ll 10^{15}$ m, meaning that bound closed orbits are expected. Applied to the solar system, we present the equation of motion of the planet, then solve it both analytically and numerically. Making use of the analytical expression of the orbit, we estimate the Yukawa strength α and find it to be larger than the nominal value (10^{-8}) adopted in previous studies, in that it is of order ($\alpha = 10^{-4} - 10^{-5}$) for the terrestrial planets (Mercury, Venus, earth, Mars, and Pluto) and even larger ($\alpha = 10^{-3}$) for the giant planets (Jupiter, Saturn, Uranus, and Neptune). Taking the inputs (r_{min}, v_{mas}, e) observed by NASA, we analyse the orbits analytically and numerically for both the estimated and nominal values of α and determine the corresponding trajectories. For each obtained orbit, we recalculate the characterizing parameters ($r_{min}, r_{max}, a, b, e$) and compare their values according to the potential (Newton with/without Yukawa correction) and method (analytical and/or numerical) used. When compared to the observational data, we conclude that the path correction due to Yukawa correction is on the order of up to 80 million km (20 million km) as the maximum deviation occurring for Neptune (Pluto) for a nominal (estimated) value of α.

Keywords: gravitational two-body problem; Yukawa potential; closed orbit

Citation: Hasan, N.A.; Joudieh, N.; Chamoun, N. Dynamics and Stability of the Two-Body Problem with Yukawa Correction to Newton's Gravity, Revisited and Applied Numerically to the Solar System. *Universe* **2023**, *9*, 45. https://doi.org/10.3390/universe9010045

Academic Editor: Kazuharu Bamba

Received: 31 October 2022
Revised: 5 January 2023
Accepted: 6 January 2023
Published: 10 January 2023

1. Introduction

The past several years have witnessed a resurgence of interest in experimental testing of gravity, particularly in the possibility of deviations from the predictions of Newtonian gravity, which is considered an excellent approximation of General Relativity (GR) on large distance scales [1]. Many theoretical models suggest the existence of a new and relatively weak intermediate-range force coexisting with gravity such that the net resulting interaction behaves as a new correction to the potentials defining the gravitational field. It is known [2] that there are only two types of central potentials, namely, the Newton $1/r$ and Harmonic r^2 potentials, where any finite motion of an object leads to a closed path subject to this central potential (Bertrand's theorem). There are 'exceptions' to this statement, in the sense that there might be closed-bound trajectories for a central potential different from the Newtonian and Harmonic, which have been studied in [3,4]. In this contribution, we revisit the effect of Yukawa correction to the gravitational force over large distances.

Theories of massive gravity [5,6] that add a mass term to the graviton (the carrier of gravity) have raised wide interest, and the Yukawa potential is the popular parametrization of such theories. Actually, many works describing deviations from Newton's inverse square law have addressed Yukawa-type correction. Assuming that gravity is exerted by exchanges of gravitons, it is clear that a test for the graviton mass (μ_g) is to ask whether

the Newton potential $(1/r)$ shows any evidence of dying at large distances because of Yukawa exponential cutoff $(e^{-\mu_g r})$. Beginning in the 1970s [7], bounds on the mass of the graviton $(\mu_g \leq 1.1 \times 10^{-29}$ eV) have been used to place a bound on its Compton wavelength, considered as a distance scale for Yukawa correction $(\lambda \sim \frac{2\pi}{\mu_g} \geq 3.7$ MPc). The authors of [8] provided a bound on the Yukawa range (λ) in the order of $(10^1 - 10^4$ AU), corresponding to $(\mu_g \leq 10^{-24})$ eV.

Theories such as Scalar-Tensor-Vector Gravity Theory [9] predict a Yukawa-like fifth force. The authors of [10] showed that screened modified gravity can suppress the fifth force in dense regions, allowing theories to evade the solar system and laboratory tests of the weak equivalence principle. In [11], an extended theory of gravity with a modified potential including post-Newtonian terms called 'vacuum bootstrapped Newtonian gravity' for which expansion is different from that of Yukawa correction, was subjected to solar system tests through a procedure which was applied to Yukawa corrections at the Galactic center [12]. No significant deviations from GR were found.

In [13], a Keplerian-type parametrization was shown as a solution of the equations of motion for a Yukawa-type potential between two bodies. In fact, the two-body solution for alternative theories yielded a strong constraint for the solar system [14,15], whereas several analyses of Yukawa potential for a two-body system in different contexts were carried out as well [16,17]. The orbit of a single particle moving under Yukawa potential was studied in [18], and precessing ellipse-type orbits were observed. In [19], it was noted that modified gravity with a Yukawa-like long-range potential was (un)successful on astrophysical scales (in the solar system), whereas an analysis of the Yukawa potential in $f(R)$ gravity was provided in [20]. The work of [21] showed that a Yukawa fifth force is expected to be sub-dominant in satellite dynamics and space geodesy experiments as long as they are performed at altitudes greater than a few hundred kilometres. The Yukawa strength was estimated in [22] to be $(\alpha < 10^{-5}$–$10^{-8})$ for distances of order 10^9 cm, whereas the use of laser data from LAGEOS satellites yielded a constraint on α of the order of 10^{-12}.

In this article, we build on work from [23], in which the dynamics and stability of the two-body problem with a Newtonian potential corrected by a Yukawa term were explored. In particular, we have reproduced their analytical results and applied them to the study of all the planets of our solar system. Analytically, by solving the planet equation of motion one finds an elliptical trajectory, which can be obtained numerically using the Runge–Kutta method. Starting from the observed values of the perihelion distance and velocity (r_{min}, v_{max}) and of the trajectory eccentricity e stated in NASA public results [24][1], it is possible to determine the ellipsis equation and estimate for the Yukawa corrected potential, i.e., the Yukawa strength α. This estimated value, or another nominal value taken from other studies, can then be used to either draw the analytical trajectory and recalculate the characterizing parameters (the shortest (longest) distance to the Sun $r_{min}(r_{max})$, the semi major (minor) axis $a(b)$, and the eccentricity e), or to solve the equations of motion with the Yukawa-corrected potential numerically in order to check the closedness of the resulting trajectory, the characteristics of which are to be reevaluated again. Later, we compared these results to those calculated for the Keplerian motion of planets subject to the pure Newtonian potential, and showed the compatibility of the results with the observational NASA data.

More specifically, for the two-body system (planet–sun), the Newtonian potential is provided by

$$V_N(r) = -\frac{Gm_pM_\odot}{r} \tag{1}$$

where $G = 6.674 \times 10^{-11} \frac{\mathrm{Nm}^2}{\mathrm{Kg}^2}$ is the gravitational Newton constant and m_p $(M_\odot)$ is the planet (sun) mass. With a Yukawa correction, the gravitational potential becomes

$$V(r) = -\frac{Gm_pM_\odot}{r}\left(1 + \alpha e^{-\frac{r}{\lambda}}\right) = V_N(r) + V_{Yk}(r) \tag{2}$$

where V_{Yk} is the Yukawa correction to the Newtonian potential and α (λ) represents the strength (range) of the Yukawa correction. Previous studies [23,25] have provided the nominal values ($\alpha = 10^{-8} (\lambda = 10^3 \text{AU} = 10^{15}$ m). However, our estimations result in a larger order of magnitude for the Yukawa strength: $\alpha \sim 10^{-4} - 10^{-5}$ for the terrestrial planets (Mercury, Venus, Earth, Mars, and Pluto) and $\alpha \sim 10^{-3}$ for the giant planets (Jupiter, Saturn, Uranus, and Neptune), which are in line with [13].

We found that for the estimated α, the maximum deviation from observed data (which increases the further the planet is (20 million km for Pluto)), is less than that of the nominal value of α (80 million km for Neptune), which is plausible considering that the estimation of α is performed by identifying the factor containing it in the observational data.

For each of the nominal and estimated values of α, we analysed the planet trajectories both analytically and numerically. Analytics-wise, we started from the NASA observational data (r_{min}, v_{max}, e) and reconstructed the closed ellipse trajectory, for which we then re-evaluated the characteristics ($r_{min}, r_{max}, a, b, e$) and compared it with both the pure Newton case and the observational data. Numerics-wise, α determines the potential under which the planet moves; thus, one can solve the equations of motion numerically using the Runge–Kutta method, taking as initial conditions the observed data of (r_{min}, v_{max}) to check whether closed trajectories are obtained in excellent agreement with the elliptical shapes, for which the evaluated characteristics can then be compared to the pure Newtonian case, the analytical method results, and the observed data.

The rest of this manuscript is organized as follows. In Section 2, we revise the system dynamics using Hamilton's method. In Section 3, we state the types of stability and determine the one corresponding to the system under study. In Section 4, and following [23], we discuss Bertrand's theorem and obtain the analytical solution to the equation of motion. Finally, in Section 5 we obtain the obtained approximative analytical results for the study of the solar system planets in order to estimate the Yukawa strength and re-determine the trajectory characteristics for both the estimated and nominal values of α, as well as to solve the equations numerically. The results of comparing the analytical/numerical outputs with the observed data according to the used potential are presented in form of plots for all the planets, whereas the corresponding tables are provided in the appendices. We end the paper with our conclusions in Section 6.

2. Hamiltonian Formulation

We start with the Hamiltonian $H = T + V$, where T is the kinetic energy of both masses and V is the gravitational potential energy:

$$\mathcal{H} = \frac{\vec{p}_1^2}{2m_p} + \frac{\vec{p}_2^2}{2M_\odot} - \frac{K}{|\vec{r}_2 - \vec{r}_1|}\left(1 + \alpha e^{-\frac{|\vec{r}_2 - \vec{r}_1|}{\lambda}}\right) \tag{3}$$

where $\vec{r}_i, (\vec{v}_i), i = 1, 2$ are the positions (velocities) of the two masses with corresponding momenta $p_1 = M_\odot v_1, p_2 = m_p v_2$, $K = G m_p M_\odot$. Changing to the center of mass frame (c.o.m), with

$$\vec{r}_1 = +\frac{m_p}{m_p + M_\odot}\vec{r} = +\frac{\mu}{M_\odot}\vec{r} + \vec{R} \quad , \quad \vec{r}_2 = -\frac{M_\odot}{m_p + M_\odot}\vec{r} = -\frac{\mu}{m_p}\vec{r} + \vec{R} \tag{4}$$

$$\vec{r} = \vec{r}_1 - \vec{r}_2 \quad , \quad \vec{R} = \frac{M_\odot \vec{r}_1 + m_p \vec{r}_2}{m_p + M_\odot} \tag{5}$$

$$\vec{v}_1 = \dot{\vec{R}} + \frac{\mu}{M_\odot}\vec{v} \quad , \quad \vec{v}_2 = \dot{\vec{R}} + \frac{-\mu}{m_p}\vec{v} \tag{6}$$

$$\vec{v} = \dot{\vec{r}} \quad , \quad \vec{p} = \mu \vec{v}, \tag{7}$$

$$\ddot{\vec{R}} = \vec{0} \quad , \quad \mu \ddot{\vec{r}} = M_\odot \ddot{\vec{r}}_1 = -m_p \ddot{\vec{r}}_2, \tag{8}$$

we have

$$\mathcal{H} = \frac{1}{2}(M_\odot + m_p)\dot{\vec{R}}^2 + H \quad : \quad H = \frac{p^2}{2\mu} - \frac{K}{r}\left(1 + \alpha e^{-\frac{r}{\lambda}}\right) \tag{9}$$

Here, we have defined $\mu = \frac{m_p M_\odot}{m_p + M_\odot}$ as the reduced mass of the system and $r = |\vec{r}|$. We switch to polar coordinates in the c.o.m to obtain

$$H = \frac{1}{2\mu}\left(p_r^2 + \frac{p_\varphi^2}{r^2}\right) - \frac{K}{r}\left(1 + \alpha e^{-\frac{r}{\lambda}}\right) \tag{10}$$

From the canonical equations [26] $\dot{q}_i = \left(\frac{\partial H}{\partial p_i}\right)$, $\dot{p}_i = -\left(\frac{\partial H}{\partial q_i}\right)$ and because the Hamiltonian is cyclic in φ (i.e., it does not depend explicitly on φ), we have

$$\dot{\varphi} = \frac{\partial H}{\partial p_\varphi} = \frac{p_\varphi}{\mu r^2} \tag{11}$$

$$\dot{p}_\varphi = -\frac{\partial H}{\partial \varphi} = 0 \Rightarrow p_\varphi = \mu r^2 \dot{\varphi} = \ell = \text{constant} \tag{12}$$

where ℓ is the angular momentum of the two-body system; therefore, Hamilton's equations for r become

$$\dot{r} = \frac{\partial H}{\partial p_r} = \frac{p_r}{\mu} \tag{13}$$

$$\dot{p}_r = -\frac{\partial H}{\partial r} = \frac{\ell^2}{\mu r^3} - \frac{K}{r^2}\left[1 + \alpha\left(1 + \frac{r}{\lambda}\right)e^{-\frac{r}{\lambda}}\right] \tag{14}$$

Again, because $H(t) = H(t_0) = h$ is constant during the motion of the masses [26] and because $p_r^2 = \mu^2 \dot{r}^2 \geq 0$, we have a lower bound for the total energy of the system:

$$h \geq \frac{\ell^2}{2\mu r^2} - \frac{K}{r}\left(1 + \alpha e^{-\frac{r}{\lambda}}\right) \tag{15}$$

The right hand side of Equation (15) is defined to be the "reduced potential", which is common in the Kepler problem moving from two degrees of freedom to only one (with the Yukawa correction):

$$V_{red}(r) = \frac{\ell^2}{2\mu r^2} - \frac{K}{r}\left(1 + \alpha e^{-\frac{r}{\lambda}}\right) \tag{16}$$

One can draw the function for a fixed ℓ given the allowed regions of motion (see Figure 1); note that $\mu > 0, \lambda > 0$ and $\alpha > 0$.

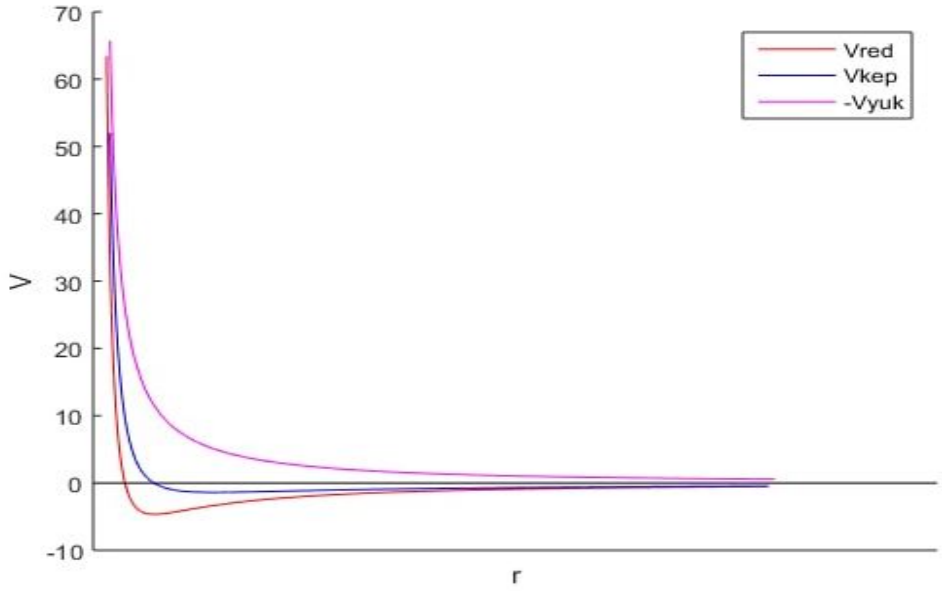

Figure 1. The reduced potential (red line) for fixed angular momentum (Equation (16)). The pink line denotes the magnitude of the purely Yukawa term ($\left|-\frac{\alpha K}{r}e^{-\frac{r}{\lambda}}\right|$), whereas the blue line represents the Keplerian reduced potential, i.e., Equation (16), without the Yukawa term.

3. The Linearization Matrix

Following [27], in order to determine the stability of the equilibrium points of the system, we must form a matrix differential equation using the system equations of motion (Hamilton's Equations (13) and (14) for r, p). The linear system has the following form:

$$\frac{d}{dt}\begin{pmatrix} r \\ p_r \end{pmatrix} = \begin{pmatrix} f(r,p) \\ g(r,p) \end{pmatrix} = \begin{pmatrix} f_0 \\ g_0 \end{pmatrix}_{eq} + \begin{pmatrix} \frac{\partial f}{\partial r} & \frac{\partial f}{\partial p_r} \\ \frac{\partial g}{\partial r} & \frac{\partial g}{\partial p_r} \end{pmatrix}\begin{pmatrix} r \\ p_r \end{pmatrix}$$
$$\text{where } f(r,p_r) = \frac{p_r}{\mu}, \quad g(r,p_r) = \frac{\ell^2}{\mu r^3} - \frac{K}{r^2}\left[1+\alpha\left(1+\frac{r}{\lambda}\right)e^{-\frac{r}{\lambda}}\right] \tag{17}$$

Considering that $\lambda = 10^{15}$ m for orbits of sizes comparable to the solar system's dimensions [28], we can assume that $\frac{r}{\lambda}$ is small enough to use Taylor expansion on the exponential and ignore the terms of $\left(\frac{r^2}{\lambda^2}\right)$, leading to

$$e^{-\frac{r}{\lambda}} \approx 1 - \frac{r}{\lambda} + O\left(\frac{r^2}{\lambda^2}\right) \approx 1 - \frac{r}{\lambda} \tag{18}$$

Thus,

$$g(r,p_r) = \frac{\ell^2}{\mu r^3} - \frac{K}{r^2}\left[1+\alpha\left(1+\frac{r}{\lambda}\right)\left(1-\frac{r}{\lambda}\right)\right] \approx \frac{\ell^2}{\mu r^3} - \frac{K}{r^2}(1+\alpha),$$

with the Yukawa effect within this approximation being limited to replacing K with $K(1+\alpha)$, which tells us that the potential shape remains Newtonian $(1/r)$; thus, according to Bertrand's theorem, every bound trajectory is closed for small r/λ. This fact can be seen directly from Equation (16); compared to the Keplerian potential, with a small shift in addition to the replacement $(K \to K(1+\alpha))$, which does not interfere in the equations of motion, it provides

$$V_{red}(r) \approx \frac{\ell^2}{2\mu r^2} - \frac{K}{r}(1+\alpha) + \frac{K\alpha}{\lambda}. \tag{19}$$

Consequently, the Jacobian matrix takes the form

$$\begin{pmatrix} \dot{r} \\ \dot{p}_r \end{pmatrix} = \begin{pmatrix} 0 & \frac{1}{\mu} \\ \frac{-3\ell^2}{\mu r^4} + \frac{2K}{r^3}(1+\alpha) & 0 \end{pmatrix} \begin{pmatrix} r \\ p_r \end{pmatrix} \tag{20}$$

where terms of the order $O\left(\frac{r^2}{\lambda^2}\right)$ are ignored and where the equilibrium point $(r, p_r)_{eq}$ satisfies $f_{eq}(r, p_r) = g_{eq}(r, p_r) = 0$. We can determine r at equilibrium using (Equation (14)) to reach the leading order:

$$r_{eq} = \frac{\ell^2}{\mu K(1+\alpha)} \tag{21}$$

We can now test for stability by choosing values of $(\alpha, \mu, K, \ell, \lambda)$ and finding the eigenvalues of the Jacobian matrix (20) after substituting the equilibrium solution found above (Equation (21)). Recall that the eigenvalues β_1, β_2 are found by solving the following equation:

$$\det|J - \beta I_{2\times 2}| = 0 \tag{22}$$

with $I_{2\times 2}$ referring to the 2×2 identity matrix. Thus, we have

$$\begin{vmatrix} -\beta & \frac{1}{\mu} \\ \frac{-3\ell^2}{\mu r^4} + \frac{2K}{r^3}(1+\alpha) & -\beta \end{vmatrix} = 0. \tag{23}$$

The characteristic equation (the eigenvalue equation) becomes

$$\beta_{1,2} = \frac{1}{2}\left(\tau \pm \sqrt{\tau^2 - 4\Delta}\right) \tag{24}$$

$$\tau = \text{trace}(J) = 0 \tag{25}$$

$$\Delta = \det(J) = \frac{\mu^2 K^4 (1+\alpha)^4}{\ell^6} \tag{26}$$

Following [29], the stability is determined by the sign of the eigenvalues. Because $\Delta > 0$, we have the following cases:

- $\tau < 0, \tau^2 - 4\Delta > 0 \Rightarrow (r_0, p_{r0})$, a stable node
- $\tau < 0, \tau^2 - 4\Delta < 0 \Rightarrow (r_0, p_{r0})$, a stable spiral
- $\tau > 0, \tau^2 - 4\Delta > 0 \Rightarrow (r_0, p_{r0})$, an unstable node
- $\tau > 0, \tau^2 - 4\Delta < 0 \Rightarrow (r_0, p_{r0})$, an unstable spiral
- $\tau = 0, \tau^2 - 4\Delta < 0 \Rightarrow (r_0, p_{r0})$, a neutrally stable center (which is our case)

Actually, the stability refers to how the solution behaves near the equilibrium point, in that unstable solutions grow to infinity, whereas stable solutions tend to zero. Furthermore, the imaginary cases are the ones resulting in bound orbital solutions (specifically, the center case), whereas the stable and unstable imaginary cases have bound solutions tending towards or away from zero.

4. Stability and Bertrand's Theorem

First, we rewrite the eigenvalue equation in the form

$$\beta^2 + \frac{\mu^2 K^4 (1+\alpha)^4}{\ell^6} = 0, \tag{27}$$

leading to

$$\beta = \pm i \frac{\mu K^2 (1+\alpha)^2}{\ell^3} \tag{28}$$

Note that we can study the case for a purely Newtonian Potential by letting $\alpha \to 0$. Similarly, by ignoring the terms derived from the Newtonian potential, we can single out

the pure Yukawa contribution. In these two extreme cases, the characteristic equations becomes

$$\text{Pure Newtonian: } \beta^2 + \frac{\mu^2 K^4}{\ell^6} = 0 \tag{29}$$

$$\text{Pure Yukawa: } \beta^2 + \frac{\mu^2 K^4 \alpha^4}{\ell^6} = 0 \tag{30}$$

resulting in

$$\text{Pure Newtonian: } \beta = \pm i \frac{\mu K^2}{\ell^3} \tag{31}$$

$$\text{Pure Yukawa: } \beta = \pm i \frac{\mu K^2 \alpha^2}{\ell^3} \tag{32}$$

Thus, the equilibrium points for the purely Newtonian, the purely Yukawa, and the Newton plus Yukawa potentials remain center solutions. This implies that the motion remains restricted to ellipses about the equilibrium point; thus, orbits near the equilibrium point are possible (further away from the equilibrium point, we would have unbounded solutions, as Figure 1 shows). This proves that for small r/λ we have stable closed orbits.

For the Keplerian orbit equation, this can be written as

$$\frac{d^2 u}{d\varphi^2} + u = -\frac{\mu}{\ell^2} \frac{d}{du} V\left(\frac{1}{u}\right) \tag{33}$$

where $u = 1/r$ denotes the Binet transformation providing the following differential equation for small r/λ:

$$\frac{d^2 u}{d\varphi^2} + u = +\frac{\mu K}{\ell^2}(1 + \alpha) \tag{34}$$

the solution of which is provided by

$$u(\varphi) = \frac{1}{r} = A[1 + e\cos(\varphi - \varphi_0)] : A = \frac{\mu K}{\ell^2}(1 + \alpha) \tag{35}$$

with e the eccentricity of the orbit. The purely Newtonian and purely Yukawa cases follow respectively from (34):

$$\text{Newtonoian: } u(\varphi) = \frac{1}{r} = \frac{\mu K}{\ell^2}[1 + e\cos(\varphi - \varphi_0)] \tag{36}$$

$$\text{Purely Yukawa: } u(\varphi) = \frac{1}{r} = \frac{\mu K \alpha}{\ell^2}[1 + e\cos(\varphi - \varphi_0)] \tag{37}$$

Finally, in order to satisfy Bertrand's theorem, the following condition should be satisfied:

$$\left.\frac{d^2 V_{red}(r)}{dr^2}\right|_{r=r_0} > 0 \tag{38}$$

where the reduced potential is provided by (16). With the approximations of (Equation 18)) and ignoring terms of order $O\left(\frac{r^2}{\lambda^2}\right)$, this condition becomes

$$\left.\frac{d^2 V_{red}(r)}{dr^2}\right|_{r=r_0} = \frac{\mu^2 K^4 (1 + \alpha)^4}{\ell^6} > 0 \tag{39}$$

which is true, because $\alpha, \mu, K, \ell > 0$, in general and in the special cases of the purely Newtonian ($\alpha = 0$) and purely Yukawa potentials. This shows that the Yukawa plus Newtonian potential satisfies Bertrand's theorem for small r/λ.

5. Application to the Solar System

We now present our results, consisting of first determining the parameters of the models $(r_{min}, r_{max}, a, b, e)$ by comparing the previous approximative analytical solutions with the NASA data. Then, we solve the equations of motion numerically using Matlab and the fourth-order Runge–Kutta method with no approximation, allowing for comparison with the analytical solutions and the observed NASA data. We applied this for all the planets of the solar system. For each sun–planet pair, we used the following values: $M_\odot = 1.9885 \times 10^{30}$ kg, $\alpha_{\text{nominal}} = 10^{-8}$, $\lambda = 10^{15}$ m. Table 1 lists the initial conditions used in the analytical and numerical calculations (the period τ is used only in the numerical solution to determine the corresponding 'step'):

Table 1. Initial conditions used in the calculations, where m_p denotes the planet mass, τ the orbit period, r_{min} the perihelion, and v_{max} the perihelion velocity.

	Mercury	**Venus**	**Earth**	**Mars**	**Jupiter**	**Saturn**	**Uranus**	**Neptune**	**Pluto**
m_p ($\times 10^{24}$ kg)	0.3302	4.8673	5.9722	0.64169	1898.13	568.32	86.811	102.409	0.01303
τ (days)	87.969	224.701	365.256	686.98	4332.589	10,832.33	30,685.4	60189	90,560
r_{min} ($\times 10^6$ km)	0.046	0.10748	0.147095	0.20665	0.740595	1.357554	2.732696	4.47105	4.434987
v_{max} ($\times 10^3$ m/s)	58.98	35.26	30.29	26.5	13.72	10.18	7.11	5.5	6.1
eccentricity	0.20563	0.00677	0.01671	0.09341	0.04839	0.05415	0.04717	0.00859	0.24881

5.1. Analytical Method

The analytical ellipsis equation is of the form

$$\frac{1}{r} \equiv u \quad = \quad \frac{a}{b^2}(1 + e\cos\varphi), \tag{40}$$

where, for a y-axis perpendicular to the polar axis in the orbit plane,

$$r_{min} = a(1-e) \quad , \quad r_{max} = a(1+e), \tag{41}$$

$$e = \frac{c}{a} = \sqrt{1 - \frac{b^2}{a^2}} \quad : \quad c^2 = a^2 - b^2, \tag{42}$$

$$a = \frac{r_{min} + r_{max}}{2} \quad , \quad b = \frac{y_{max} - y_{min}}{2} \tag{43}$$

Thus, analytically we can start with (r_{min}, v_{max}, e), observed by NASA in [24], to compute[2]

$$a = \frac{r_{min}}{1-e} \quad , \quad b = a\sqrt{1-e^2}, \tag{44}$$

and estimate the strength of α from

$$\frac{\mu K}{\ell^2}(1+\alpha) = \frac{a}{b^2} \quad \text{using} \quad \ell = r_{min} v_{max}. \tag{45}$$

When the analytical equation is determined, we can then plot the trajectory and recompute the characteristics $(r_{min}, r_{max}, a, b, e)$ using Equations (41) and (42). We call this procedure the "analytical-α-estimated" approach.

In addition, we can use the nominal value of $\alpha = 10^{-8}$ in Equation (40), where ℓ, e are taken from the observed data, to re-evaluate $(r_{min}, r_{max}, a, b, e)$ from

$$a = \frac{1}{A(1-e^2)}, \quad A = \frac{\mu K(1+\alpha)}{\ell^2}, \quad b = \frac{1}{A\sqrt{1-e^2}}. \tag{46}$$

We call this procedure the "analytical-α-nominal" approach, which can be considered as a method with three inputs (α, ℓ, e) instead of the three inputs (r_{min}, v_{max}, e) used in the other approach.

5.2. Numerical Method

Here, we use the fourth-order Runge–Kutta method to solve the Newton's law equation of motion in the c.o.m frame numerically with initial conditions taken from NASA. Thus, we solve the following equations:

$$\ddot{\vec{r}}_1 = Gm_p \frac{\vec{r}_2 - \vec{r}_1}{r^3} \quad \text{, Newton,} \quad \ddot{\vec{r}}_2 = GM_\odot \frac{\vec{r}_1 - \vec{r}_2}{r^3} = -\frac{M_\odot}{m_p}\ddot{\vec{r}}_1, \tag{47}$$

$$\ddot{\vec{r}}_1 = Gm_p \left[(1 + \alpha e^{-\frac{r}{\lambda}}) \frac{1}{r} + \frac{\alpha}{\lambda} e^{-\frac{r}{\lambda}} \right] \frac{\vec{r}_2 - \vec{r}_1}{r^2} \quad \text{, Newton+Yukawa,} \quad \ddot{\vec{r}}_2 = -\frac{M_\odot}{m_p}\ddot{\vec{r}}_1, \tag{48}$$

under the initial conditions provided by the NASA data (r_{min}, v_{max}):

$$\vec{r}_1(t = t_{min}) = \frac{m_p}{m_p + M_\odot}\vec{r}_{min} \quad , \quad \vec{v}_1(t = t_{min}) = \frac{m_p}{m_p + M_\odot}\vec{v}_{max}, \tag{49}$$

$$\vec{r}_2(t = t_{min}) = -\frac{M_\odot}{m_p + M_\odot}\vec{r}_{min} \quad , \quad \vec{v}_2(t = t_{min}) = -\frac{M_\odot}{m_p + M_\odot}\vec{v}_{max}. \tag{50}$$

After the trajectory is solved numerically, we check that it is closed, as Figure 2 shows for both the purely Newton and purely Yukawa corrections (as the differences are not visible on the figure scale containing all the planets). For each obtained orbit, we recalculate the corresponding characteristics $(r_{min}, r_{max}, a, b, e)$.

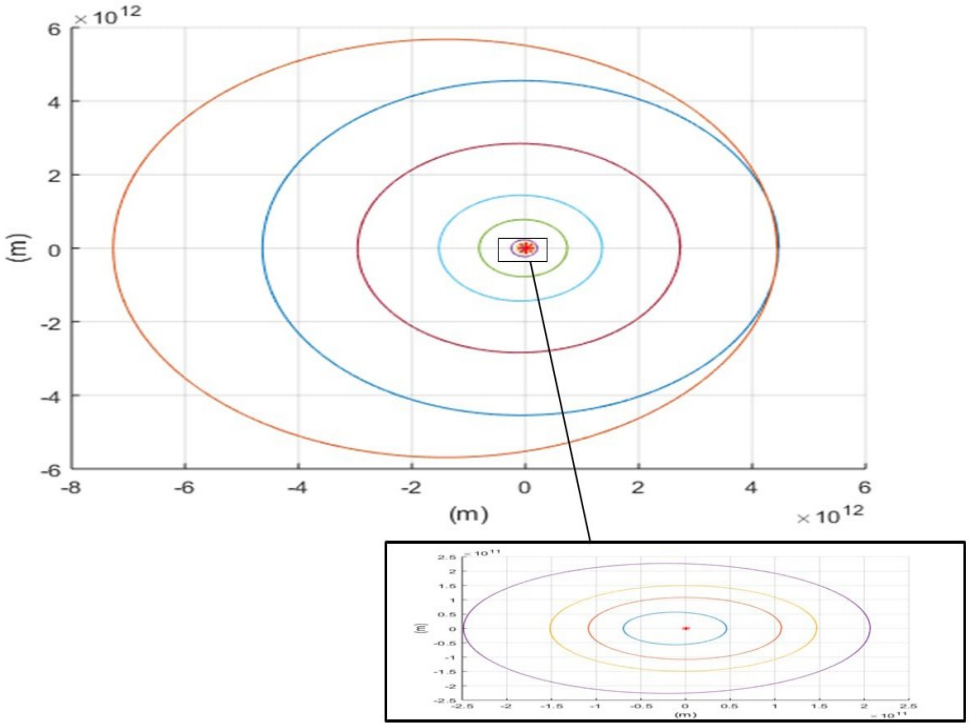

Figure 2. Closed - bound planet trajectories with and without Yukawa correction with nominal strength α.

5.3. Results

In the Tables of Appendix A (from Tables A1–A18), we report the calculated characteristics of the resulting trajectories for all the planets in the solar system corresponding to the pure Newton and Newton corrected with Yukawa potentials in both the analytical and the numerical approaches. The odd (even) numbered tables correspond to the nominal (estimated) Yukawa strength α. The number of moons of each planet is determined according to [30]. Below, we explain the meanings of the symbols used in the tables:

- N_{num}: numerical calculations using the Newtonian potential
- N_{anal}: analytical calculations using the Newtonian potential
- $R_N = \frac{N_{num}}{N_{anal}}\%$: percentage ratio of the numerical to the analytical results for the Newton potential
- $(N+YK)_{num}$: numerical calculations using the modified potential
- $(N+YK)_{anal}$: analytical calculations using the modified potential
- $R_{N+YK} = \frac{(N+YK)_{num}}{(N+YK)_{anal}}\%$: percentage ratio of the numerical to the analytical results for the modified potential
- $R^{N-Obs}_{num} = N_{num}/Obs\%$: percentage ratio of the numerical results to the observed results using the Newtonian potential
- $R^{N-Obs}_{anal} = N_{anal}/Obs$ %: percentage ratio of the analytical results to the observed results using the Newtonian potential
- $R^{YK-Obs}_{num} = (N+YK)_{num}/Obs$ %: percentage ratio of the numerical results to the observed results using the modified potential
- $R^{YK-Obs}_{anal} = (N+YK)_{anal}/Obs$ %: percentage ratio of the analytical results to the observed results using the modified potential.

In order to summarize the findings of the Tables, in Figure 3 we present plots showing the deviation from unity of the ratio between two quantities of the following for each planet and at every polar angle, allowing for comparison of the effects of the considered potential (Newton vs. Newton + Yuakawa) and/or the used method (numerical vs. analytical) and/or the Yukawa strength determination (nominal vs. estimated):

- $rn(num)$, representing the trajectory equation of the numerical approach with Newton potential
- $rn(anl)$, representing the trajectory equation of the analytical approach with Newton potential
- $ryk(num)$, representing the trajectory equation of the numerical approach with Newton+Yukawa potential and nominal α
- $ryk(anl)$, representing the trajectory equation of the analytical approach with Newton+Yukawa potential and nominal α
- $ryka(num)$, representing the trajectory equation of the numerical approach with Newton+Yukawa potential and estimated α
- $ryka(anl)$, representing the trajectory equation of the analytical approach with Newton+Yukawa potential and estimated α.

It can be seen that several ratios (e.g., the dashed red and sky blue) do coincide near zero deviation from one, meaning that there is no tangible effect when adding the Yukawa correction in either the analytic or numeric method as long as one takes the nominal value of α. Furthermore, local extremums for the deviations from unity at polar angles that are multiples of $\pi/2$ can be noted as a generic feature in many plots. We can interpret the large values of the deviations for the nearest (Mercury) and farthest (Pluto) planets in that for the former, the perturbative effect of solar wind, which is important approaching the sun, was not taken into consideration; for the latter, the accumulated gravitational screening effects of the other planets and their moons, which were not considered in the study, become important, especially for a small sized-planetoid such as Pluto.

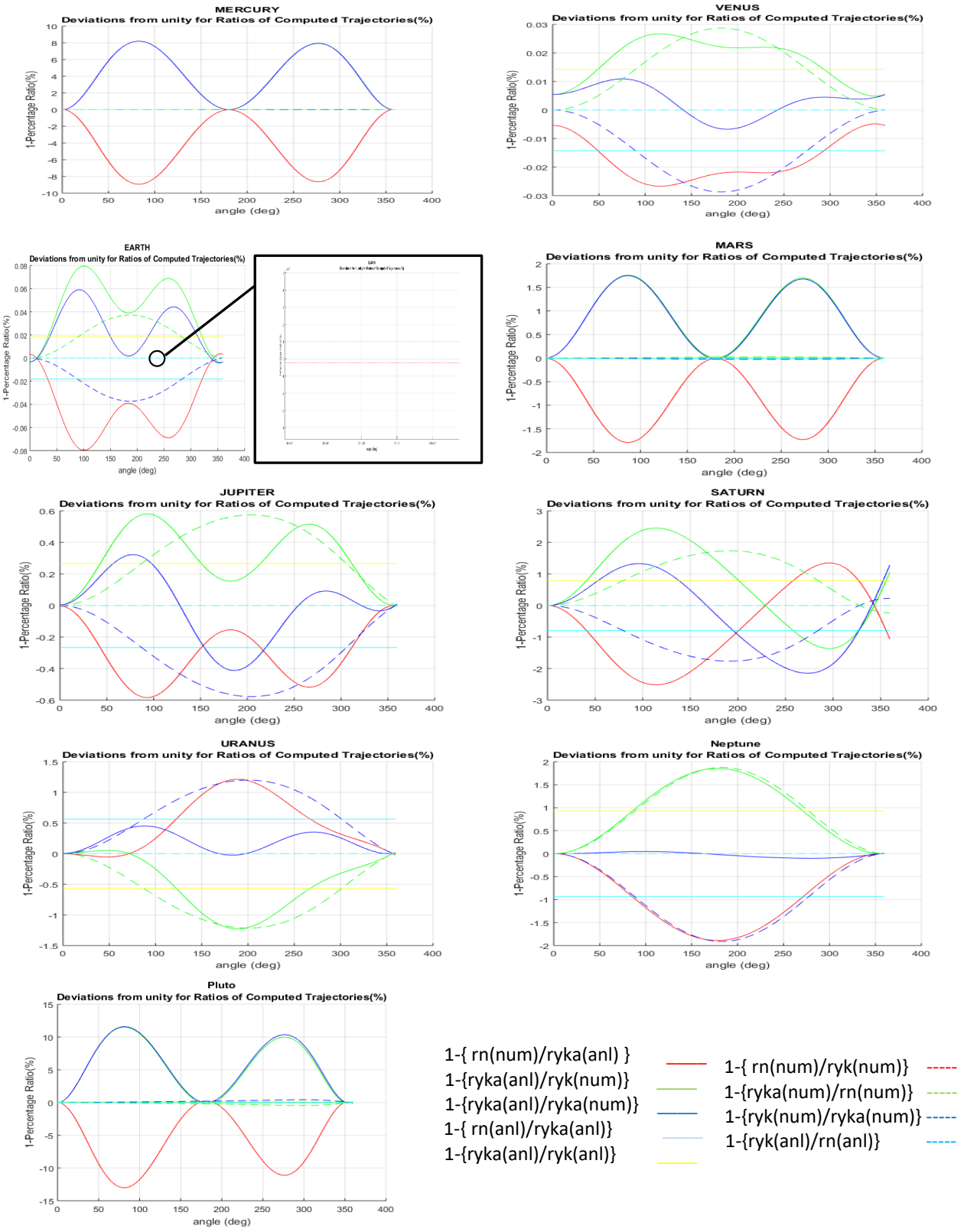

Figure 3. Deviation from unity of ratios of the computed trajectories at each polar angle according to the considered potential (Newton vs. Newton + Yukawa) and/or the used method (numerical vs. analytical) and/or the Yukawa strength determination (nominal vs. estimated). The zoomed region shows, for the generic case of one planet (Earth), that the dashed red and sky blue curves are very near each other; the same applies to the green and blue curves in the case of Mercury.

In order to show the effects of the separating distance effect, we should compute the absolute deviations from observed data for each planet. In Appendix B, Tables A19 and A20 (Tables A21 and A22) report the deviation from observation for each planet, r_{max}, r_{min}, respectively, in the case of nominal (estimated) α. We summarize these findings in Figure 4.

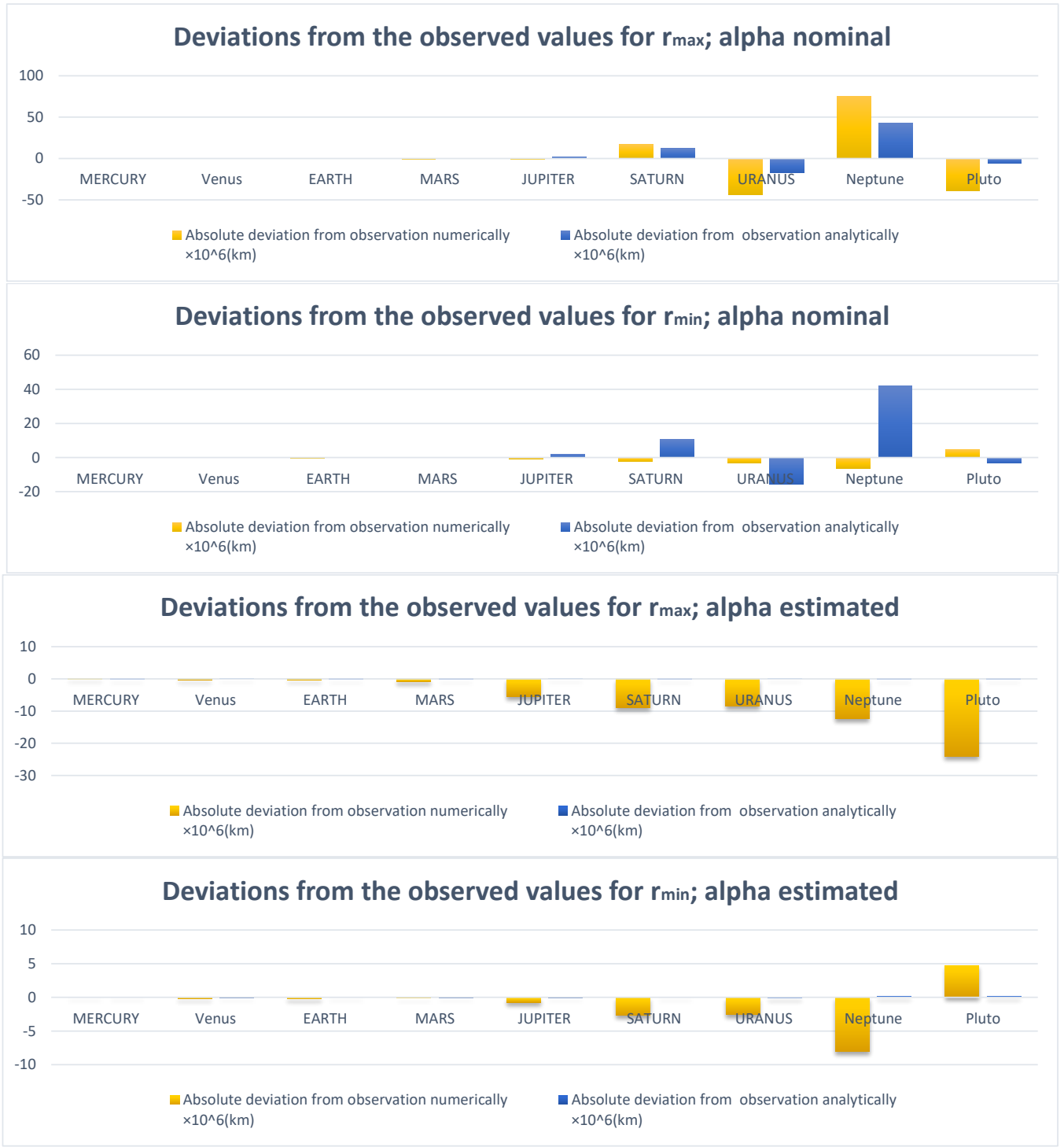

Figure 4. Absolute deviations from observed data for each planet according to the used method (numerical vs. analytical) and/or the Yukawa strength determination (nominal vs. estimated).

It can be seen that the agreement between the numerical and analytical solutions is excellent in both estimated and nominal α cases. Though the deviations due to Yukawa correction are not large, it should be noted that:

1. For estimated α:
   - r_{max}-deviation: the numerical deviation is larger by about 10^3 times the analytical deviation. In general, it increases the further out the planet is, and reaches a maximum of order (-25 million km) (less than the observed value) for Pluto.
   - r_{min}-deviation: again, the numerical deviation is larger by about (10^1–10^2)-order of magnitude than the analytical deviation, and is largest for Neptune (-8 million km); however, it reverses sign and becomes ($+5$ million km) more than the observation for Pluto.
2. For nominal α:
   - r_{max}-deviation: the numerical deviation is larger than the analytical deviation, though they are of the same order, reaching a maximum of $+80$ ($+40$) million km for Neptune using the numerical (analytical) method. For Pluto and Uranus, we obtain (-40) million km using the numerical method (less than observed).
   - r_{min}-deviation: the analytical deviation is larger, and sometimes reverses sign compared to the numerical deviation. For example, for Neptune the analytical approach provides a deviation of (+40 million km) from observation, whereas the numerical approach provides a deviation of -5 million km (less than the observed value).

Actually, the disagreements with observations are due to several reasons; the first is physical in nature, in that it results from neglecting the perturbation due to third bodies, or more generally, the effect of natural satellites such as moons or asteroids. In addition, we did not take into account the physical effects of either the radiation or the solar wind. Moreover, the results were obtained as a two-body problem; hence, the movement of more distant planets might have been be affected by planets closer to the sun, which can be present in the higher orders of expansion even if they are not in the dominant term. The second factor lies on the computational side, and concerns the numerical method used, the value of the step size, and the high sensitivity of the problem to the initial conditions. It should be mentioned that, for the analytical solution, we restricted our study to the leading order, neglecting higher orders in the expansion of exponentials, whereas for the numerical solution the entire exponential was considered.

6. Summary and Conclusions

In this work, we followed [23] and used Hamilton's formulation in order to obtain the differential equation of motion and the path equation for gravitational two-body systems. The developments were carried out in the case of the pure Newtonian potential, the Newtonian corrected with Yukawa potential, and the pure Yukawa potential. As in [23], we reviewed the stability problem, constructed the linearization matrix, and tested the stability of the system for Yukawa correction, finding that it is of a central solution type, which implies stable solutions near the fixed point. We repeated the=is analysis for a purely Yukawa force and found similar results, and confirmed that the modified potential obeys Bertrand's theorem.

Then, we determined the parameter set corresponding to the planets of the solar system, starting from the observed (r_{min}, v_{max}, e) and estimating α. For estimated and nominal values of α, we determined the characteristics of the trajectories both numerically and analytically and compared the methods with the observed data. We explained the extent to which these results are consistent with the observational data, presenting the absolute deviation from observation in the form of histograms. The results included an upper deviation of order 80 million km for Neptune using nominal α and 20 million km for Pluto using estimated α.

Author Contributions: All authors contributed equally to this work. All authors have read and agreed to the published version of the manuscript.

Funding: This research received no external funding.

Institutional Review Board Statement: Not applicable.

Informed Consent Statement: Informed consent was obtained from all subjects involved in the study.

Acknowledgments: N. Chamoun acknowledges support from the ICTP-Associate program, from the Humboldt Foundation, and from the CAS-PIFI scholarship.

Conflicts of Interest: The authors declare no conflict of interest.

Appendix A. Tables of Calculated/Observed Parameters of the Planets

Table A1. The values of the calculated and observational astronomical parameters, for nominal α, of the planet Mercury, whose number of moons is 0.

Mercury	r_{min} **($\times 10^6$ km)**	r_{max} **($\times 10^6$ km)**	a **($\times 10^6$ km)**	b **($\times 10^6$ km)**	**Eccentricity**
N_{num}	46	69.832	57.916	56.67679158	0.205744228
N_{anal}	47	72.043	59.756	58.47840586	0.205646344
$R_N = \frac{N_{num}}{N_{anal}}\%$	97	96.930	96.921	96.91918025	99.95242442
$(N+YK)_{num}$	46	69.831	57.916	56.67678243	0.205738221
$(N+YK)_{anal}$	47	72.043	59.756	58.47840528	0.205646344
$R_{N+YK} = \frac{(N+YK)_{num}}{(N+YK)_{anal}}\%$	97	96.930	96.921	96.91916556	99.95534277
Observation	46	69.818	57.909	_____	0.20563069
$R^{N-Obs}_{num} = N_{num}/Obs\ \%$	100	99.980	99.988	_____	99.94481595
$R^{N-Obs}_{anal} = N_{anal}/Obs\ \%$	97	96.911	96.909	_____	99.9923879
$R^{YK-Obs}_{num} = (N+YK)_{num}/Obs\ \%$	100	99.981	99.988	_____	99.94773407
$R^{YK-Obs}_{anal} = (N+YK)_{anal}/Obs\ \%$	97	96.911	96.909	_____	99.9923879
nominal $\alpha = 10^{-8}$					

Table A2. The values of the calculated and observational astronomical parameters, for estimated α, of the planet Mercury, whose number of moons is 0.

Mercury	r_{min} **(**$\times 10^6$ **km)**	r_{max} **(**$\times 10^6$ **km)**	a **(**$\times 10^6$ **km)**	b **(**$\times 10^6$ **km)**	**Eccentricity**
N_{num}	46	69.623	57.826	56.65144795	0.2022
N_{anal}	46	69.819	57.912	56.67470066	0.2056
$R_N = \frac{N_{num}}{N_{anal}}\%$	100	99.719	99.851	99.95897162	98.3743
$(N+YK)_{num}$	46	69.613	57.820	56.64729064	0.2022
$(N+YK)_{anal}$	46	69.815	57.908	56.6714469	0.2056
$R_{N+YK} = \frac{(N+YK)_{num}}{(N+YK)_{anal}}\%$	100	99.711	99.847	99.9573749	98.3408
Observation	46	69.818	57.909	_____	0.2056
$R^{N-Obs}_{num} = N_{num}/Obs\ \%$	100	99.721	99.856	_____	98.3817
$R^{N-Obs}_{anal} = N_{anal}/Obs\ \%$	100	100.001	100.005	_____	100.0075
$R^{YK-Obs}_{num} = (N+YK)_{num}/Obs\ \%$	100	99.706	99.847	_____	98.3482
$R^{YK-Obs}_{anal} = (N+YK)_{anal}/Obs\ \%$	100	99.995	99.999	_____	100.0075
estimated $\alpha = 5.741444131301954 \times 10^{-5}$					

Table A3. The values of the calculated and observational astronomical parameters, for nominal α, of the planet Venus, whose number of moons is 0.

Venus	r_{min} **(**$\times 10^6$ **km)**	r_{max} **(**$\times 10^6$ **km)**	a **(**$\times 10^6$ **km)**	b **(**$\times 10^6$ **km)**	**Eccentricity**
N_{num}	107.30	108.689	107.99	107.9982364	0.0044
N_{anal}	107.48	108.961	108.22	108.2222348	0.0072
$R_N = \frac{N_{num}}{N_{anal}}\%$	99.83	99.750	99.79	99.79301998	60.8187
$(N+YK)_{num}$	107.30	108.689	107.99	107.9982353	0.0044
$(N+YK)_{anal}$	107.48	108.961	108.22	108.2222337	0.0072
$R_{N+YK} = \frac{(N+YK)_{num}}{(N+YK)_{anal}}\%$	99.83	99.750	99.79	99.79301998	60.8189
Observation	107.48	108.941	108.21	_____	0.0068
$R^{N-Obs}_{num} = N_{num}/Obs\ \%$	99.83	99.769	99.80	_____	64.7150
$R^{N-Obs}_{anal} = N_{anal}/Obs\ \%$	100.00	100.018	100.01	_____	106.4063
$R^{YK-Obs}_{num} = (N+YK)_{num}/Obs\ \%$	99.83	99.769	99.80	_____	64.7152
$R^{YK-Obs}_{anal} = (N+YK)_{anal}/Obs\ \%$	100.00	100.018	100.01	_____	106.4063
nominal $\alpha = 10^{-8}$					

Table A4. The values of the calculated and observational astronomical parameters, for estimated α, of the planet Venus, whose number of moons is 0.

Venus	r_{min} **(**$\times 10^6$ **km)**	r_{max} **(**$\times 10^6$ **km)**	a **(**$\times 10^6$ **km)**	b **(**$\times 10^6$ **km)**	**Eccentricity**
N_{num}	107.30	108.689	107.99	107.9982364	0.0044
N_{anal}	107.48	108.961	108.22	108.2222348	0.0072
$R_N = \frac{N_{num}}{N_{anal}}\%$	99.83	99.750	99.79	99.79301998	60.8187
$(N+YK)_{num}$	107.30	108.658	107.98	107.9821956	0.0045
$(N+YK)_{anal}$	107.47	108.945	108.20	108.2068155	0.0072
$R_{N+YK} = \frac{(N+YK)_{num}}{(N+YK)_{anal}}\%$	99.84	99.736	99.78	99.79241613	63.0300
Observation	107.48	108.941	108.21	_____	0.0068
$R^{N-Obs}_{num} = N_{num}/Obs\ \%$	99.83	99.769	99.80	_____	64.7150
$R^{N-Obs}_{anal} = N_{anal}/Obs\ \%$	100.00	100.018	100.01	_____	106.4063
$R^{YK-Obs}_{num} = (N+YK)_{num}/Obs\ \%$	99.83	99.740	99.78	_____	67.0680
$R^{YK-Obs}_{anal} = (N+YK)_{anal}/Obs\ \%$	99.99	100.004	99.99	_____	106.4063
estimated $\alpha = 1.424988220126711 \times 10^{-4}$					

Table A5. The values of the calculated and observational astronomical parameters, for nominal α, of the planet Earth, whose number of moons is 0.

Earth	r_{min} **(**$\times 10^6$ **km)**	r_{max} **(**$\times 10^6$ **km)**	a **(**$\times 10^6$ **km)**	b **(**$\times 10^6$ **km)**	**Eccentricity**
N_{num}	146.884	151.7	149.336	149.319847	0.0156
N_{anal}	147.126	152.1	149.625	149.6034965	0.0168
$R_N = \frac{N_{num}}{N_{anal}}\%$	99.835	99.7	99.806	99.81039915	92.5721
$(N+YK)_{num}$	146.884	151.7	149.336	149.3198455	0.0156
$(N+YK)_{anal}$	147.126	152.1	149.625	149.603495	0.0168
$R_{N+YK} = \frac{(N+YK)_{num}}{(N+YK)_{anal}}\%$	99.835	99.7	99.806	99.81039915	92.5720
Observation	147.095	152.1	149.598	_____	0.0167
$R^{N-Obs}_{num} = N_{num}/Obs\ \%$	99.8572	99.7	99.825	_____	93.5903
$R^{N-Obs}_{anal} = N_{anal}/Obs\ \%$	99.978	99.9	99.981	_____	98.9120
$R^{YK-Obs}_{num} = (N+YK)_{num}/Obs\ \%$	99.857	99.7	99.825	_____	93.5902
$R^{YK-Obs}_{anal} = (N+YK)_{anal}/Obs\ \%$	99.978	99.9	99.981	_____	98.9120
nominal $\alpha = 10^{-8}$					

Table A6. The values of the calculated and observational astronomical parameters, for estimated α, of the planet Earth, whose number of moons is 0.

Earth	r_{min} **(**$\times 10^6$ **km)**	r_{max} **(**$\times 10^6$ **km)**	a **(**$\times 10^6$ **km)**	b **(**$\times 10^6$ **km)**	**Eccentricity**
N_{num}	146.884	151.7	149.336	149.319847	0.0156
N_{anal}	147.126	152.1	149.625	149.6034965	0.0168
$R_N = \frac{N_{num}}{N_{anal}}\%$	99.835	99.7	99.806	99.81039915	92.5721
$(N+YK)_{num}$	146.883	151.7	149.307	149.2910008	0.0154
$(N+YK)_{anal}$	147.099	152.0	149.597	149.5762082	0.01688
$R_{N+YK} = \frac{(N+YK)_{num}}{(N+YK)_{anal}}\%$	99.853	99.7	99.805	99.80932302	91.4700
Observation	147.095	152.1	149.598	_____	0.0167
$R^{N-Obs}_{num} = N_{num}/Obs\ \%$	99.8572	99.7	99.825	_____	93.5903
$R^{N-Obs}_{anal} = N_{anal}/Obs\ \%$	99.978	99.9	99.981	_____	98.9120
$R^{YK-Obs}_{num} = (N+YK)_{num}/Obs\ \%$	99.856	99.7	99.805	_____	92.4761
$R^{YK-Obs}_{anal} = (N+YK)_{anal}/Obs\ \%$	100.003	99.9	99.999	_____	101.0999
estimated $\alpha = 1.824376359731428 \times 10^{-4}$					

Table A7. The values of the calculated and observational astronomical parameters, for nominal α, of the planet Mars, whose number of moons is 0.

Mars	r_{min} **(**$\times 10^6$ **km)**	r_{max} **(**$\times 10^6$ **km)**	a **(**$\times 10^6$ **km)**	b **(**$\times 10^6$ **km)**	**Eccentricity**
N_{num}	206.57	248.480	227.52	226.6509159	0.0898
N_{anal}	206.64	249.277	227.96	226.9631182	0.0935
$R_N = \frac{N_{num}}{N_{anal}}\%$	99.96	99.680	99.80	99.8624436	96.0965
$(N+YK)_{num}$	206.57	248.480	227.52	226.6509134	0.0898
$(N+YK)_{anal}$	206.64	249.277	227.96	226.9631159	0.0935
$R_{N+YK} = \frac{(N+YK)_{num}}{(N+YK)_{anal}}\%$	99.96	99.680	99.80	99.86244351	96.0965
Observation	206.65	249.261	227.94	_____	0.0935
$R^{N-Obs}_{num} = N_{num}/Obs\ \%$	99.96	99.687	99.81	_____	96.1252
$R^{N-Obs}_{anal} = N_{anal}/Obs\ \%$	99.99	100.006	100.01	_____	100.0298
$R^{YK-Obs}_{num} = (N+YK)_{num}/Obs\ \%$	99.96	99.687	99.81	_____	96.1252
$R^{YK-Obs}_{anal} = (N+YK)_{anal}/Obs\ \%$	99.99	100.006	100.01	_____	100.0298
nominal $\alpha = 10^{-8}$					

Table A8. The values of the calculated and observational astronomical parameters, for estimated α, of the planet Mars, whose number of moons is 0.

Mars	r_{min} **(**$\times 10^6$ **km)**	r_{max} **(**$\times 10^6$ **km)**	a **(**$\times 10^6$ **km)**	b **(**$\times 10^6$ **km)**	**Eccentricity**
N_{num}	206.57	248.480	227.52	226.6509159	0.0898
N_{anal}	206.64	249.277	227.96	226.9631182	0.0935
$R_N = \frac{N_{num}}{N_{anal}}\%$	99.96	99.680	99.80	99.8624436	96.0965
$(N+YK)_{num}$	206.57	248.425	227.49	226.6249874	0.0897
$(N+YK)_{anal}$	206.62	249.252	227.93	226.9402451	0.0935
$R_{N+YK} = \frac{(N+YK)_{num}}{(N+YK)_{anal}}\%$	99.97	99.668	99.80	99.86108339	95.9861
Observation	206.65	249.261	227.94	_____	0.0935
$R^{N-Obs}_{num} = N_{num}/Obs\ \%$	99.96	99.687	99.81	_____	96.1252
$R^{N-Obs}_{anal} = N_{anal}/Obs\ \%$	99.99	100.006	100.01	_____	100.0298
$R^{YK-Obs}_{num} = (N+YK)_{num}/Obs\ \%$	99.96	99.664	99.80	_____	96.0147
$R^{YK-Obs}_{anal} = (N+YK)_{anal}/Obs\ \%$	99.98	99.996	99.99	_____	100.0298
estimated $\alpha = 1.007889331583467 \times 10^{-4}$					

Table A9. The values of the calculated and observational astronomical parameters, for nominal α, of the planet Jupiter, whose number of moons is 0.

Jupiter	r_{min} **(**$\times 10^6$ **km)**	r_{max} **(**$\times 10^6$ **km)**	a **(**$\times 10^6$ **km)**	b **(**$\times 10^6$ **km)**	**Eccentricity**
N_{num}	739.902	815.533	777.717	776.9190412	0.0469
N_{anal}	742.542	818.568	780.555	779.626266	0.04873
$R_N = \frac{N_{num}}{N_{anal}}\%$	99.644	99.629	99.636	99.65275352	96.3711
$(N+YK)_{num}$	739.902	815.533	777.717	776.9190329	0.0469
$(N+YK)_{anal}$	742.542	818.568	780.555	779.6262582	0.0487
$R_{N+YK} = \frac{(N+YK)_{num}}{(N+YK)_{anal}}\%$	99.644	99.629	99.636	99.65275345	96.3711
Observation	740.595	816.363	778.479	_____	0.0487
$R^{N-Obs}_{num} = N_{num}/Obs\ \%$	99.906	99.898	99.902	_____	96.4399
$R^{N-Obs}_{anal} = N_{anal}/Obs\ \%$	100.262	100.270	100.266	_____	100.0714
$R^{YK-Obs}_{num} = (N+YK)_{num}/Obs\ \%$	99.906	99.898	99.902	_____	96.4399
$R^{YK-Obs}_{anal} = (N+YK)_{anal}/Obs\ \%$	100.262	100.270	100.266	_____	100.0714
nominal $\alpha = 10^{-8}$					

Table A10. The values of the calculated and observational astronomical parameters, for estimated α, of the planet Jupiter, whose number of moons is 0.

Jupiter	r_{min} **(**$\times 10^6$ **km)**	r_{max} **(**$\times 10^6$ **km)**	a **(**$\times 10^6$ **km)**	b **(**$\times 10^6$ **km)**	**Eccentricity**
N_{num}	739.902	815.533	777.717	776.9190412	0.0469
N_{anal}	742.542	818.568	780.555	779.626266	0.04873
$R_N = \frac{N_{num}}{N_{anal}}\%$	99.644	99.629	99.636	99.65275352	96.3711
$(N+YK)_{num}$	739.837	810.932	775.385	774.6852056	0.0441
$(N+YK)_{anal}$	740.567	816.390	778.478	777.5526264	0.0487
$R_{N+YK} = \frac{(N+YK)_{num}}{(N+YK)_{anal}}\%$	99.901	99.331	99.602	99.63122486	90.6263
Observation	740.595	816.363	778.479	_____	0.0487
$R^{N-Obs}_{num} = N_{num}/Obs\ \%$	99.906	99.898	99.902	_____	96.4399
$R^{N-Obs}_{anal} = N_{anal}/Obs\ \%$	100.262	100.270	100.266	_____	100.0714
$R^{YK-Obs}_{num} = (N+YK)_{num}/Obs\ \%$	99.897	99.334	99.602	_____	90.6911
$R^{YK-Obs}_{anal} = (N+YK)_{anal}/Obs\ \%$	99.996	100.003	99.999	_____	100.0714
estimated $\alpha = 2.666880127522 \times 10^{-3}$					

Table A11. The values of the calculated and observational astronomical parameters, for nominal α, of the planet Saturn, whose number of moons is 0.

Saturn	r_{min} **(**$\times 10^6$ **km)**	r_{max} **(**$\times 10^6$ **km)**	a **(**$\times 10^6$ **km)**	b **(**$\times 10^6$ **km)**	**Eccentricity**
N_{num}	1355.461	1523.344	1439.403	1437.455093	0.055
N_{anal}	1368.378	1518.496	1443.437	1441.481829	0.052
$R_N = \frac{N_{num}}{N_{anal}}\%$	99.056	100.319	99.720	99.72065302	106.042
$(N+YK)_{num}$	1355.461	1523.344	1439.403	1437.455078	0.055
$(N+YK)_{anal}$	1368.378	1518.496	1443.437	1441.481815	0.052
$R_{N+YK} = \frac{(N+YK)_{num}}{(N+YK)_{anal}}\%$	99.056	100.319	99.720	99.72065294	106.042
Observation	1357.554	1506.527	1432.041	_____	0.052
$R^{N-Obs}_{num} = N_{num}/Obs\ \%$	99.845	101.116	100.514	_____	106.081
$R^{N-Obs}_{anal} = N_{anal}/Obs\ \%$	100.797	100.794	100.795	_____	100.036
$R^{YK-Obs}_{num} = (N+YK)_{num}/Obs\ \%$	99.845	101.116	100.514	_____	106.081
$R^{YK-Obs}_{anal} = (N+YK)_{anal}/Obs\ \%$	100.797	100.794	100.795	_____	100.036
nominal $\alpha = 10^{-8}$					

Table A12. The values of the calculated and observational astronomical parameters, for estimated α, of the planet Saturn, whose number of moons is 0.

Saturn	r_{min} **(**$\times 10^6$ **km)**	r_{max} **(**$\times 10^6$ **km)**	a **(**$\times 10^6$ **km)**	b **(**$\times 10^6$ **km)**	**Eccentricity**
N_{num}	1355.461	1523.344	1439.403	1437.455093	0.055
N_{anal}	1368.378	1518.496	1443.437	1441.481829	0.052
$R_N = \frac{N_{num}}{N_{anal}}\%$	99.056	100.319	99.720	99.72065302	106.042
$(N+YK)_{num}$	1354.869	1497.652	1426.261	1424.954776	0.046
$(N+YK)_{anal}$	1357.574	1506.507	1432.040	1430.100672	0.052
$R_{N+YK} = \frac{(N+YK)_{num}}{(N+YK)_{anal}}\%$	99.800	99.412	99.596	99.64017246	89.244
Observation	1357.554	1506.527	1432.041	_____	0.052
$R^{N-Obs}_{num} = N_{num}/Obs\ \%$	99.845	101.116	100.514	_____	106.081
$R^{N-Obs}_{anal} = N_{anal}/Obs\ \%$	100.797	100.794	100.795	_____	100.036
$R^{YK-Obs}_{num} = (N+YK)_{num}/Obs\ \%$	99.802	99.410	99.596	_____	89.277
$R^{YK-Obs}_{anal} = (N+YK)_{anal}/Obs\ \%$	100.001	99.998	99.999	_____	100.036
estimated $\alpha = 7.958291053541 \times 10^{-3}$					

Table A13. The values of the calculated and observational astronomical parameters, for nominal α, of the planet Uranus, whose number of moons is 0.

Uranus	r_{min} **(**$\times 10^6$ **km)**	r_{max} **(**$\times 10^6$ **km)**	a **(**$\times 10^6$ **km)**	b **(**$\times 10^6$ **km)**	**Eccentricity**
N_{num}	2729.595	2957.44	2843.519	2841.649275	0.0381
N_{anal}	2717.213	2984.63	2850.921	2847.766462	0.0469
$R_N = \frac{N_{num}}{N_{anal}}\%$	100.455	99.08	99.740	99.78519352	81.2504
$(N+YK)_{num}$	2729.595	2957.44	2843.519	2841.649245	0.0381
$(N+YK)_{anal}$	2717.213	2984.63	2850.921	2847.766434	0.0469
$R_{N+YK} = \frac{(N+YK)_{num}}{(N+YK)_{anal}}\%$	100.455	99.08	99.740	99.78519344	81.2504
Observation	2732.696	3001.39	2867.043	_____	0.0469
$R^{N-Obs}_{num} = N_{num}/Obs\ \%$	99.886	98.53	99.179	_____	81.3684
$R^{N-Obs}_{anal} = N_{anal}/Obs\ \%$	99.433	99.44	99.437	_____	100.1452
$R^{YK-Obs}_{num} = (N+YK)_{num}/Obs\ \%$	99.886	98.53	99.179	_____	81.3684
$R^{YK-Obs}_{anal} = (N+YK)_{anal}/Obs\ \%$	99.433	99.44	99.437	_____	100.1452
nominal $\alpha = 10^{-8}$					

Table A14. The values of the calculated and observational astronomical parameters, for estimated α, of the planet Uranus, whose number of moons is 0.

Uranus	r_{min} **(**$\times 10^6$ **km)**	r_{max} **(**$\times 10^6$ **km)**	a **(**$\times 10^6$ **km)**	b **(**$\times 10^6$ **km)**	**Eccentricity**
N_{num}	2729.595	2957.44	2843.519	2841.649275	0.0381
N_{anal}	2717.213	2984.63	2850.921	2847.766462	0.0469
$R_N = \frac{N_{num}}{N_{anal}}\%$	100.455	99.08	99.740	99.78519352	81.2504
$(N+YK)_{num}$	2730.116	2992.91	2861.516	2858.935401	0.0441
$(N+YK)_{anal}$	2732.578	3001.50	2867.042	2863.869614	0.0469
$R_{N+YK} = \frac{(N+YK)_{num}}{(N+YK)_{anal}}\%$	99.909	99.71	99.807	99.82770818	94.0932
Observation	2732.696	3001.39	2867.043	_____	0.0469
$R^{N-Obs}_{num} = N_{num}/Obs\ \%$	99.886	98.53	99.179	_____	81.3684
$R^{N-Obs}_{anal} = N_{anal}/Obs\ \%$	99.433	99.44	99.437	_____	100.1452
$R^{YK-Obs}_{num} = (N+YK)_{num}/Obs\ \%$	99.905	99.71	99.807	_____	94.2299
$R^{YK-Obs}_{anal} = (N+YK)_{anal}/Obs\ \%$	99.995	100.00	99.999	_____	100.1452
estimated $\alpha = -5.622864957252 \times 10^{-3}$					

Table A15. The values of the calculated and observational astronomical parameters, for nominal α, of the planet, Neptune whose number of moons is 0.

Neptune	r_{min} **(**$\times 10^6$ **km)**	r_{max} **(**$\times 10^6$ **km)**	a **(**$\times 10^6$ **km)**	b **(**$\times 10^6$ **km)**	**Eccentricity**
N_{num}	4464.81	4634.099	4549.454	4548.810665	0.0177
N_{anal}	4512.97	4601.381	4557.176	4556.953752	0.0097
$R_N = \frac{N_{num}}{N_{anal}}\%$	98.93	100.711	99.830	99.82130416	180.8744
$(N+YK)_{num}$	4464.81	4634.098	4549.454	4548.810617	0.0177
$(N+YK)_{anal}$	4512.97	4601.381	4557.176	4556.953706	0.0097
$R_{N+YK} = \frac{(N+YK)_{num}}{(N+YK)_{anal}}\%$	98.93	100.711	99.830	99.82130411	180.8743
Observation	4471.05	4558.857	4514.953	_____	0.0097
$R^{N-Obs}_{num} = N_{num}/Obs\ \%$	99.86	101.650	100.764	_____	182.6474
$R^{N-Obs}_{anal} = N_{anal}/Obs\ \%$	100.93	100.932	100.935	_____	100.9802
$R^{YK-Obs}_{num} = (N+YK)_{num}/Obs\ \%$	99.86	101.650	100.764	_____	182.6473
$R^{YK-Obs}_{anal} = (N+YK)_{anal}/Obs\ \%$	100.93	100.932	100.935	_____	100.9802
nominal $\alpha = 10^{-8}$					

Table A16. The values of the calculated and observational astronomical parameters, for estimated α, of the planet Neptune, whose number of moons is 0.

Neptune	r_{min} **(**$\times 10^6$ **km)**	r_{max} **(**$\times 10^6$ **km)**	a **(**$\times 10^6$ **km)**	b **(**$\times 10^6$ **km)**	**Eccentricity**
N_{num}	4464.81	4634.099	4549.454	4548.810665	0.0177
N_{anal}	4512.97	4601.381	4557.176	4556.953752	0.0097
$R_N = \frac{N_{num}}{N_{anal}}\%$	98.93	100.711	99.830	99.82130416	180.8744
$(N+YK)_{num}$	4463.01	4546.479	4504.745	4504.517794	0.0096
$(N+YK)_{anal}$	4471.15	4558.747	4514.952	4514.73215	0.0097
$R_{N+YK} = \frac{(N+YK)_{num}}{(N+YK)_{anal}}\%$	99.81	99.730	99.773	99.77375499	98.6587
Observation	4471.05	4558.857	4514.953	_____	0.0097
$R^{N-Obs}_{num} = N_{num}/Obs\ \%$	99.86	101.650	100.764	_____	182.6474
$R^{N-Obs}_{anal} = N_{anal}/Obs\ \%$	100.93	100.932	100.935	_____	100.9802
$R^{YK-Obs}_{num} = (N+YK)_{num}/Obs\ \%$	99.82	99.728	99.773	_____	99.6259
$R^{YK-Obs}_{anal} = (N+YK)_{anal}/Obs\ \%$	100.00	99.997	99.999	_____	100.9802
estimated $\alpha = 9.351961741362 \times 10^{-3}$					

Table A17. The values of the calculated and observational astronomical parameters, for nominal α, of the planet Pluto, whose number of moons is 0.

Pluto	r_{min} **(**$\times 10^6$ **km)**	r_{max} **(**$\times 10^6$ **km)**	a **(**$\times 10^6$ **km)**	b **(**$\times 10^6$ **km)**	**Eccentricity**
N_{num}	4439.709	7265.423	5852.566	5684.326067	0.2397
N_{anal}	4431.722	7298.614	5865.168	5687.267307	0.2444
$R_N = \frac{N_{num}}{N_{anal}}\%$	100.180	99.545	99.785	99.94828377	98.0832
$(N+YK)_{num}$	4439.709	7265.423	5852.566	5684.325992	0.2397
$(N+YK)_{anal}$	4431.722	7298.614	5865.168	5687.26725	0.2444
$R_{N+YK} = \frac{(N+YK)_{num}}{(N+YK)_{anal}}\%$	100.180	99.545	99.785	99.94828346	98.0832
Observation	4434.987	7304.326	5869.656	_____	0.2444
$R^{N-Obs}_{num} = N_{num}/Obs\ \%$	100.106	99.467	99.708	_____	98.0882
$R^{N-Obs}_{anal} = N_{anal}/Obs\ \%$	99.926	99.921	99.923	_____	100.0051
$R^{YK-Obs}_{num} = (N+YK)_{num}/Obs\ \%$	100.106	99.467	99.708	_____	98.0882
$R^{YK-Obs}_{anal} = (N+YK)_{anal}/Obs\ \%$	99.926	99.921	99.923	_____	100.0051
nominal $\alpha = 10^{-8}$					

Table A18. The values of the calculated and observational astronomical parameters, for estimated α, of the planet Pluto, whose number of moons is 0.

Pluto	r_{min} **($\times 10^6$ km)**	r_{max} **($\times 10^6$ km)**	a **($\times 10^6$ km)**	b **($\times 10^6$ km)**	**Eccentricity**
N_{num}	4439.709	7265.423	5852.566	5684.326067	0.2397
N_{anal}	4431.722	7298.614	5865.168	5687.267307	0.2444
$R_N = \frac{N_{num}}{N_{anal}}\%$	100.180	99.545	99.785	99.94828377	98.0832
$(N+YK)_{num}$	4439.740	7280.242	5859.991	5690.112819	0.2407
$(N+YK)_{anal}$	4435.112	7304.196	5869.654	5691.616958	0.2444
$R_{N+YK} = \frac{(N+YK)_{num}}{(N+YK)_{anal}}\%$	100.104	99.672	99.835	99.97357273	98.4812
Observation	4434.987	7304.326	5869.656	_____	0.2444
$R^{N-Obs}_{num} = N_{num}/Obs\ \%$	100.106	99.467	99.708	_____	98.0882
$R^{N-Obs}_{anal} = N_{anal}/Obs\ \%$	99.926	99.921	99.923	_____	100.0051
$R^{YK-Obs}_{num} = (N+YK)_{num}/Obs\ \%$	100.107	99.670	99.835	_____	98.4862
$R^{YK-Obs}_{anal} = (N+YK)_{anal}/Obs\ \%$	100.002	99.998	99.999	_____	100.0051
	estimated $\alpha = -7.642205983339201 \times 10^{-4}$				

Appendix B. Tables of Absolute Deviations from Observation of the Planets

Table A19. Absolute deviation of r_{max} from observation with nominal α, evaluated in (10^6 km).

	R^{YK-Obs}_{num}	R^{YK-Obs}_{anal}	**Observed** r_{max}	$r^{num}_{max} - Obs$	$r^{anal}_{max} - Obs$
Mercury	99.721	100.001	69.818	−0.194	0.001
Venus	99.769	100.018	108.941	−0.251	0.020
Earth	99.794	99.984	152.100	−0.312	−0.024
Mars	99.687	100.006	249.261	−0.780	0.016
Jupiter	99.898	100.270	816.363	−0.829	2.205
Saturn	101.116	100.794	1506.527	16.817	11.969
Uranus	98.535	99.441	3001.390	−43.947	−16.759
Neptune	101.650	100.932	4558.857	75.241	42.524
Pluto	99.467	99.921	7304.326	−38.902	−5.711

Table A20. Absolute deviation of r_{min} from observation with nominal α, evaluated in (10^6 km).

	R_{num}^{YK-Obs}	R_{anal}^{YK-Obs}	**Observed** r_{min}	$r_{min}^{num} - Obs$	$r_{min}^{anal} - Obs$
Mercury	100.062	100.012	46.000	0.028	0.005
Venus	99.839	100.008	107.480	−0.172	0.009
Earth	99.857	99.978	147.095	−0.210	−0.031
Mars	99.962	99.999	206.650	−0.077	−0.001
Jupiter	99.906	100.262	740.595	−0.692	1.947
Saturn	99.845	100.797	1357.554	−2.092	10.824
Uranus	99.886	99.433	2732.696	−3.100	−15.482
Neptune	99.860	100.937	4471.050	−6.239	41.922
Pluto	100.106	99.926	4434.987	4.722	−3.264

Table A21. Absolute deviation of r_{max} from observation with estimated α, evaluated in (10^6 km).

	R_{num}^{YK-Obs}	R_{anal}^{YK-Obs}	**Observed** r_{max}	$r_{max}^{num} - Obs$	$r_{max}^{anal} - Obs$
Mercury	99.706	99.995	69.818	−0.204	−0.002
Venus	99.740	100.004	108.941	−0.282	0.004
Earth	99.757	99.997	152.100	−0.369	−0.003
Mars	99.664	99.996	249.261	−0.835	−0.008
Jupiter	99.334	100.003	816.363	−5.430	0.027
Saturn	99.410	99.998	1506.527	−8.874	−0.019
Uranus	99.717	100.003	3001.390	−8.472	0.117
Neptune	99.728	99.997	4558.857	−12.377	−0.109
Pluto	99.670	99.998	7304.326	−24.083	−0.12907

Table A22. Absolute deviation of r_{min} from observation with estimated α, evaluated in (10^6 km).

	R_{num}^{YK-Obs}	R_{anal}^{YK-Obs}	**Observed** r_{min}	$r_{min}^{num} - Obs$	$r_{min}^{anal} - Obs$
Mercury	100.062	100.006	46.000	0.028	0.002
Venus	99.838	99.994	107.480	−0.173	−0.005
Earth	99.856	100.003	147.095	−0.211	0.004
Mars	99.962	99.989	206.650	−0.077	−0.022
Jupiter	99.897	99.996	740.595	−0.757	−0.027
Saturn	99.802	100.001	1357.554	−2.684	0.020
Uranus	99.905	99.995	2732.696	−2.579	−0.117
Neptune	99.820	100.002	4471.050	−8.037	0.107
Pluto	100.107	100.002	4434.987	4.753	0.125

Notes

1. Although the standard deviations of the planetary trajectories are not quoted in the NASA public website, one can consider that the corresponding error is equal to the last digit of the quoted significant numbers. In our computations, we used the whole digits allowed by machine precision; however, the results in the tables in the appendices show only significant digits equal to those from the observed data.
2. Due to measurement errors and orbits not being perfectly elliptical, the NASA data may provide slightly different values of a when using Equation (43) or Equation (44).

References

1. Fischbach, E.; Talmadge, C.L. *The Search for Non-Newtonian Gravity*; Springer: Berlin, Germany, 1998.
2. Landau, L.D.; Lifshitz, E.M. *Course of Theoretical Physics (Mechanics)*; Pergamon Press: Oxford, UK, 1969; Volume 1, Chapter 3, Section 14, p. 32.
3. Rodriguez, I.; Brun, J.L. Closed orbits in central forces distinct from Coulomb or harmonic oscillator type. *Eur. J. Phys.* **1998**, *19*, 41–49. [CrossRef]
4. Brun, J.L.; Pacheco, A.F. On closed but non-geometrically similar orbits. *Celest. Mech. Dyn. Astr.* **2006**, *96*, 311–316. [CrossRef]
5. Hinterbichler, K. Theoretical Aspects of Massive Gravity. *Rev. Mod. Phys.* **2012**, *84*, 671. [CrossRef]
6. De Rham, C. Massive Gravity. *Living Rev. Relativ.* **2014**, *17*, 7. [CrossRef] [PubMed]
7. Goldhabert, A.S.; Nieto, M.M. Mass of the graviton. *Phys. Rev. D* **1974**, *9*, 1119. [CrossRef]
8. Dong, Y.; Shao, L.; Hu, Z.; Miaoc, X.; Wang, Z. Prospects for Constraining the Yukawa Gravity with Pulsars around Sagittarius A*. *J. Cosmol. Astropart. Phys.* **2022**, *2022*, 051. [CrossRef]
9. Moffat, J.W. Scalar-tensor-vector gravity theory. *J. Cosmol. Astropart. Phys.* **2006**, *3*, 4. [CrossRef]
10. Zhang, X.; Liu, T.; Zhao, W. Gravitational radiation from compact binary systems in screened modified gravity. *Phys. Rev. D* **2017**, *95*, 104027. [CrossRef]
11. D'Addio, A.; Casadio, R.; Giusti, A.; Laurentis, M.D. Orbits in bootstrapped Newtonian gravity. *Phys. Rev. D* **2021**, *105*, 104010. [CrossRef]
12. Monica, R.D.; de Martino, I.; Laurentis, M.D. Orbital precession of the S2 star in Scalar–Tensor–Vector Gravity. *Mon. Not. R. Astron. Soc.* **2022**, *510*, 4757–4766.
13. Benisty, D. Testing modified gravity via Yukawa potential in two body problem: Analytical solution and observational constraints. *Phys. Rev. D* **2022**, *106*, 043001. [CrossRef]
14. Banik, I.; Zhao, H. Testing gravity with wide binary stars like α Centauri. *Mon. Not. R. Astron. Soc.* **2018**, *480*, 2660. [Erratum: *Mon. Not. R. Astron. Soc.* **2019**, *482*, 3453. Erratum: *Mon. Not. R. Astron. Soc.* **2019**, *484*, 1589]. [CrossRef]
15. Yu, Q.; Zhang, F.; Lu, Y. Prospects for constraining the spin of the massive black hole at the galactic center via the relativistic motion of a surrounding star. *Astrophys. J.* **2016**, *827*, 114. [CrossRef]
16. Pricopi, D. Stability of the celestial body orbits under the influence of Yukawa potential. *Astrophys. Space Sci.* **2016**, *361*, 277. [CrossRef]
17. Edwards, J.P.; Gerber, U.; Schubert, C.; Trejo, M.A.; Weber, A. The Yukawa potential: Ground state energy and critical screening. *Prog. Theor. Exp. Phys.* **2017**, *2017*, 083A01. [CrossRef]
18. Mukherjee, R.; Sounda, S. Single particle closed orbits in Yukawa potential. *Indian J. Phys.* **2018**, *92*, 197. [CrossRef]
19. Iorio, L. Putting Yukawa-Like Modified Gravity (MOG) on the Test in the Solar System. *Sch. Res. Exch.* **2008**, *2008*, 238385. [CrossRef]
20. Laurentis, M.D.; Martino, I.D.; Lazkoz, R. Analysis of the Yukawa gravitational potential in f(R) gravity II: Relativistic periastron advance. *Phys. Rev. D* **2018**, *97*, 104068. [CrossRef]
21. Bergé, J.; Brax, P.; Pernot-Borràs, M.; Uzan, J.-P. Interpretation of geodesy experiments in non-Newtonian theories of gravity. *Class. Quant. Grav.* **2018**, *35*, 234001. [CrossRef]
22. Iorio, L. Constraints on a Yukawa gravitational potential from laser data of LAGEOS satellites. *Phys. Lett. A* **2002**, *298*, 315–318. [CrossRef]
23. Cavan, E.; Haranas, I.; Gkigkitzis, I.; Cobbett, K. Dynamics and stability of the two body problem with Yukawa correction. *Astrophys. Space Sci.* **2020**, *365*, 2. [CrossRef]
24. Available online: https://nssdc.gsfc.nasa.gov/planetary/factsheet/index.html (accessed on 5 January 2023).
25. Rujula, A. *Remnants of the Fifth Force*; CERN-TH 4466/86; Viki-Fest: Erice, Italiy, 1986.
26. Goldstein, H. *Classical Mechanics*, 2nd ed.; Addison-Wesley Publishing Company: Reading, MA, USA, 1980.
27. Meiss, J.D. *Differential Dynamical Systems*; Revised Edition; SIAM-Society for Industrial and Applied Mathematics: Philadelphia, PA, USA, 2017.
28. Fackler, O.; Van, J.T.T. EDITIONS FRONTIERES, B. P.33, 91192 Gif-sur-Yvette Cedex-France. In Proceedings of the 5th Force Neutrino Physics: Proceedings of VIIIth Moriond Workshop, Les Arcs, France, 23–30 January 1988.
29. Ross, S.L. *Differential Equations*; John Willey & Sons: New York, NY, USA, 1984; p. 661.
30. Wakker, K. *Fundamentals of Astrodynamics*; TU Delft Library: Delft, The Netherland, 2015; ISBN 9789461864192.